

Tuning optical modes in slab photonic crystal by atomic layer deposition and laser-assisted oxidation

Citation for published version (APA):

Kiravittaya, S., Lee, H. S., Balet, L. P., Li, L. H., Francardi, M., Gerardino, A., Fiore, A., Rastelli, A., & Schmidt, O. G. (2011). Tuning optical modes in slab photonic crystal by atomic layer deposition and laser-assisted oxidation. *Journal of Applied Physics*, 109(5), Article 053115. <https://doi.org/10.1063/1.3559269>

DOI:

[10.1063/1.3559269](https://doi.org/10.1063/1.3559269)

Document status and date:

Published: 01/01/2011

Document Version:

Publisher's PDF, also known as Version of Record (includes final page, issue and volume numbers)

Please check the document version of this publication:

- A submitted manuscript is the version of the article upon submission and before peer-review. There can be important differences between the submitted version and the official published version of record. People interested in the research are advised to contact the author for the final version of the publication, or visit the DOI to the publisher's website.
- The final author version and the galley proof are versions of the publication after peer review.
- The final published version features the final layout of the paper including the volume, issue and page numbers.

[Link to publication](#)

General rights

Copyright and moral rights for the publications made accessible in the public portal are retained by the authors and/or other copyright owners and it is a condition of accessing publications that users recognise and abide by the legal requirements associated with these rights.

- Users may download and print one copy of any publication from the public portal for the purpose of private study or research.
- You may not further distribute the material or use it for any profit-making activity or commercial gain
- You may freely distribute the URL identifying the publication in the public portal.

If the publication is distributed under the terms of Article 25fa of the Dutch Copyright Act, indicated by the "Taverne" license above, please follow below link for the End User Agreement:

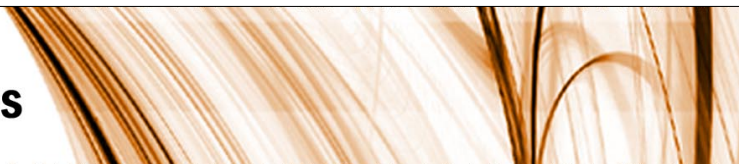
www.tue.nl/taverne

Take down policy

If you believe that this document breaches copyright please contact us at:

openaccess@tue.nl

providing details and we will investigate your claim.



Tuning optical modes in slab photonic crystal by atomic layer deposition and laser-assisted oxidation

S. Kiravittaya, H. S. Lee, L. Balet, L. H. Li, M. Francardi et al.

Citation: *J. Appl. Phys.* **109**, 053115 (2011); doi: 10.1063/1.3559269

View online: <http://dx.doi.org/10.1063/1.3559269>

View Table of Contents: <http://jap.aip.org/resource/1/JAPIAU/v109/i5>

Published by the [American Institute of Physics](http://www.aip.org).

Related Articles

High-Q aluminum nitride photonic crystal nanobeam cavities

Appl. Phys. Lett. **100**, 091105 (2012)

Magnetophotonic crystal comprising electro-optical layer for controlling helicity of light

J. Appl. Phys. **111**, 07A913 (2012)

Multimodal strong coupling of photonic crystal cavities of dissimilar size

Appl. Phys. Lett. **100**, 081107 (2012)

Highly modified spontaneous emissions in YVO₄:Eu³⁺ inverse opal and refractive index sensing application

Appl. Phys. Lett. **100**, 081104 (2012)

High quality factor two dimensional GaN photonic crystal cavity membranes grown on silicon substrate

Appl. Phys. Lett. **100**, 071103 (2012)

Additional information on *J. Appl. Phys.*


Journal Homepage: <http://jap.aip.org/>

Journal Information: http://jap.aip.org/about/about_the_journal

Top downloads: http://jap.aip.org/features/most_downloaded

Information for Authors: <http://jap.aip.org/authors>

ADVERTISEMENT

	Working @ low temperatures? Contact Janis for Cryogenic Research Equipment Click here to browse our site at www.janis.com	
-------------------------------------------------------------------------------------	---------------------------------------------------------------------------------------------------------------------------------------------------------------------------	---------------------------------------------------------------------------------------

Tuning optical modes in slab photonic crystal by atomic layer deposition and laser-assisted oxidation

S. Kiravittaya,¹ H. S. Lee,^{1,a),b)} L. Balet,² L. H. Li,² M. Francardi,³ A. Gerardino,³ A. Fiore,⁴ A. Rastelli,¹ and O. G. Schmidt¹

¹*Institute for Integrative Nanosciences, IFW Dresden, Helmholtzstr. 20, D-01069 Dresden, Germany*

²*Ecole Polytechnique Fédérale de Lausanne (EPFL), Station 3, CH-1015 Lausanne, Switzerland*

³*Institute of Photonics and Nanotechnology, CNR, via del Cineto Romano 42, 00156 Roma, Italy*

⁴*COBRA Research Institute, Eindhoven University of Technology, 5600 MB Eindhoven, The Netherlands*

(Received 27 June 2010; accepted 27 January 2011; published online 15 March 2011)

The authors experimentally investigate the effects of atomic layer deposition (ALD) and laser-assisted oxidation on the optical modes in GaAs L3 photonic crystal air-bridge cavities, using layers of InAs quantum dots as internal light source. Four distinct optical mode peaks are observed in the photonic bandgap and they show different wavelength-redshifts (0–6.5 nm) as the photonic crystal surface is coated with an Al₂O₃ layer (0–5.4 nm thick). Numerical finite-difference time-domain (FDTD) simulations can well-reproduce the experimental result and give insight into the origin of the shifts of modes with different spatial profiles. By combining the ALD coating with *in situ* laser-assisted oxidation, we are able to both redshift and blueshift the optical modes and we attribute the blueshift to the formation of a GaAs-oxide at the expense of GaAs at the interface between GaAs and the Al₂O₃ layer. This result can be quantitatively reproduced by including a GaAs-oxide layer into the FDTD model. Selective etching experiments, confirm that this GaAs-oxide layer is mainly at the interface between GaAs and Al₂O₃ layers. © 2011 American Institute of Physics. [doi:10.1063/1.3559269]

I. INTRODUCTION

Slab two-dimensional (2D) photonic crystal (PhC) nanocavities have gained much interest for their promising applications in both classical optics^{1–3} and quantum electrodynamics.^{4–6} For many applications, accurate control of the resonant wavelength in PhC nanocavities is highly desired. For instance, to accurately control the exciton-polariton state, i.e., the strong coupling between exciton state in nanostructures such as quantum dots and a photonic mode, highly refined tuning methods of either excitonic or photonic modes have to be employed. A slab PhC nanocavity consists of a defect in a PhC dielectric slab with periodically arranged air holes. The PhC nanocavity resonances can be tuned by adjusting the PhC lattice and defect geometries. However, due to fluctuations in processing parameters, the spectral position of the resonant modes cannot be predicted with the accuracy needed for some application. Recent experiments have demonstrated the possibility of irreversible tuning of the modes by using digital etching,⁵ scanning probe microscopy assisted oxidation⁶ and laser-assisted oxidation⁷ or of reversible tuning by gas absorption⁸ and laser heating.^{9,10} All these methods allow tuning of the cavity modes either on the blue or on the red side, while a complete control of the resonant wavelength requires some combination of different methods.

In this work, we investigate a combined approach to achieve permanent bidirectional tuning of PhC nanocavity

modes. Our approach is based on the combination of atomic layer deposition (ALD) of a dielectric material¹¹ and local oxidation produced by continuous wave laser irradiation of a nanocavity.⁷ While both methods have been separately described in literature, their combination to achieve bidirectional tuning on a single nanocavity has not been reported. Here, we demonstrate that the two methods can complement each other: By ALD coating we can produce large redshifts of the optical modes, while with subsequent laser-assisted oxidation we can blueshift them back to the original spectral positions. Each process step can be well understood by numerical finite-difference time-domain (FDTD) simulations.

II. EXPERIMENT AND SIMULATIONS

The samples used in this work were grown by molecular beam epitaxy and processed by standard electron beam lithography and dry etching.^{7,12} After buffer layer growth on GaAs(001) substrate, a 1.5- μ m-thick Al_{0.7}Ga_{0.3}As layer, which acts as sacrificial layer, was deposited. After that 320-nm GaAs with three layers of high density self-assembled InAs quantum dots was grown. After growth, samples were processed by 150-nm SiO₂ patterning with electron beam lithography and CHF₃ plasma etching. The triangular lattice pattern of the PhC with L3 cavities (three missing holes in a line) was transferred onto the GaAs slab by SiCl₄/O₂/Ar reactive ion etching. The sacrificial layer was then partially removed by a dip in a dilute HF solution. The PhC nanocavity is a suspended GaAs membrane with InAs quantum dot layers, which emit light at wavelengths around 1.1–1.4 μ m.

The L3 cavities have the following nominal parameters: the lattice constant a is 331 nm and the air holes have a

^{a)}Author to whom correspondence should be addressed. Electronic mail: hslee1@gist.ac.kr.

^{b)}Present address: Advanced Photonics Research Institute, Gwangju Institute of Science and Technology, Gwangju 500-712, Republic of Korea.

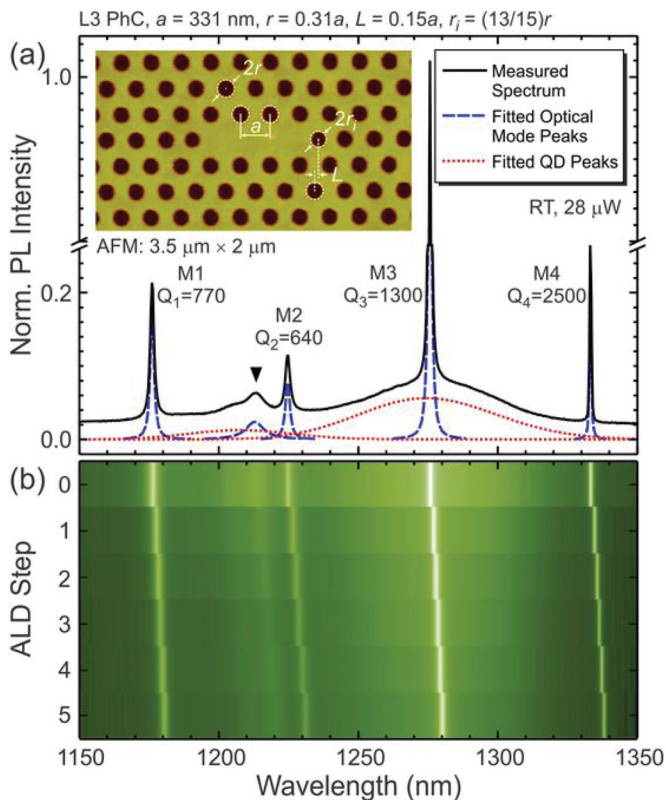


FIG. 1. (Color online) Room temperature μ -PL spectrum of as-processed L3 GaAs PhC nanocavity. The blue-dashed lines are individual fitted optical mode spectra (M1–M4). One broad mode at 1213 nm is marked by a solid triangle but is not labeled. The red dotted lines are fitted QD-related peaks. The inset is a $3.5 \times 2 \mu\text{m}^2$ AFM image of the cavity after five ALD steps with relevant structural parameters. (b) Color-coded μ -PL intensity map showing the mode peaks as a function of ALD step. One ALD step corresponds to 0.9 nm Al_2O_3 coating.

nominal radius r of $0.31a$ (filling fraction of 35%). The hole next to the cavity has a radius r_i and is displaced by a distance L away from the cavity. The inset of Fig. 1(a) shows an atomic force microscopy (AFM) image of a nanocavity with relevant design parameters. More details of the fabrication of these PhCs can be found in Refs. 7 and 12.

Atomic layer deposition on the PhC is performed with a SavannahTM (Cambridge NanoTech) ALD system. Alumina (Al_2O_3) is selected as coating material for this experiment. Each ALD step consists of 10 deposition cycles (the Al_2O_3 thicknesses 0.09 nm per cycle). The refractive index of Al_2O_3 , which was measured by ellipsometry, is 1.63. Prior to ALD coating, the sample surface was cleaned several times by HCl dips, which remove the native GaAs-oxide, thus thinning the GaAs slab and enlarging the air holes by a few nanometers.

The optical properties of the PhC cavities were characterized by standard microphotoluminescence (μ -PL) at room temperature (RT) in air.^{7,13} The excitation source is a frequency doubled continuous wave Nd:YVO₄ laser with emission wavelength of 532 nm. The laser spot with $\sim 1.5 \mu\text{m}$ diameter is focused by a $50\times$ microscope objective lens (with numerical aperture of 0.42). The same lens is used to collect the luminescence. The PL signal is subsequently dispersed by a 500-mm focal length spectrometer and finally detected by liquid-nitrogen-cooled InGaAs array.

For the laser-assisted oxidation process, a defocused laser beam ($\sim 8 \mu\text{m}$ diameter) at relatively high power (1–50

mW) is used to blueshift the optical modes. The laser excitation power is systematically increased with a constant oxidation time (20 s). Detailed experiments as well as a physical model describing this laser-assisted oxidation process have been reported in Ref. 7.

In order to interpret the results, we perform 2D FDTD simulations. Variations of the effective refractive index due to the geometric changes in the vertical direction and the changes in the lateral geometry are the main origin of the spectral shifts of the optical modes in the simulations. Due to the fact that both ALD coating and laser-assisted oxidation processes induce structural changes in both vertical and lateral directions,^{7,11} we first use a semianalytical method to calculate the variation of the effective refractive index as a function of relevant changing parameters (thicknesses of the GaAs slab, Al_2O_3 , and GaAs oxide). Details of this calculation are described in the Appendix. FDTD simulations were performed using a freely available software package.¹⁴ Built-in subpixel averaging technique¹⁵ and filter diagonalization method¹⁶ are used to improve and analyze the numerical results, respectively. For each optical mode, the excitation source is of dipole-type and the electric field is in-plane, i.e., we investigate transverse electric (TE) modes.¹⁷ The excitation and detection positions are located near the anti-node of that mode.

III. ATOMIC LAYER DEPOSITION (ALD OF PHCS)

A. L3 photonic crystal with ALD coatings

Figure 1(a) shows a normalized RT μ -PL spectrum of an as-processed L3 PhC nanocavity prior to ALD coating. The low intensity region (0–0.2) is magnified. Within the displayed spectral range (1150–1350 nm), four distinct optical mode peaks are observed at 1176, 1225, 1276, and 1333 nm. They are labeled as M1, M2, M3, and M4, respectively. In addition, a broad mode peak with relatively low intensity at 1213 nm marked by a solid triangle can be seen. All these peaks can be well fitted with Lorentzian functions (in frequency scale) and quality factors (Q) can be extracted. Each fitted optical mode peak is shown as dashed lines in the Fig. 1(a). Apart from the mode peaks, quantum dot (QD) related peaks (ground and first excited state emission) are seen in the spectrum as a broad background. These peaks can be characterized by two broad Gaussian functions as shown by the dotted lines.

Figure 1(b) shows color-coded RT μ -PL spectra as a function of ALD step. Logarithmic color-scale is used in this plot. The PL is measured at the same excitation laser power (28 μW) on the same L3 PhC after 1–5 ALD steps. Each ALD step corresponds to 0.9 nm Al_2O_3 coating. This result shows a clear redshift of all optical modes. The PL intensity as well as the Q factors of each mode does not significantly change upon coating. The AFM image shown in the inset of Fig. 1(a) was taken after 5 ALD steps.

B. Finite-difference time-domain (FDTD) simulations

For the FDTD simulation, we first adjust the structural parameters of the L3 cavity to correctly reproduce the optical mode peak positions measured on the as-processed sample [Fig. 1(a)]. The initial structure is assumed to be pure GaAs.

The thin native GaAs-oxide layer, which is usually 0.74 nm thick^{7,18} is neglected in this initial simulation. However, the GaAs-oxide layer will be considered later for interpreting the laser-assisted oxidation experiments. The best simultaneous fit of the four modes (M1–M4) is obtained when the slab GaAs thickness is reduced from the nominal 320 to 313 nm thickness and the hole radii are increased by 3.5 nm with respect to the nominal values. Without this initial adjustment, the simulations with nominal structural parameters gave the longer mode wavelengths of 13–22 nm. We attribute this discrepancy between parameters in the simulation and nominal parameters to the uncertainties in the sample processing and to the cleaning steps, which we performed prior to ALD coating. The extracted optical mode profiles corresponding to the four distinct peaks in Fig. 1(a) are shown in Fig. 2(a). Due to the fact that each mode profile has different overlap with the surrounding holes, we expect different quantitative shifts for each mode.

Figure 2(b) shows the measured and simulated mode peak shifts as a function of the ALD steps. The FDTD is performed by including an Al₂O₃ layer on all GaAs surfaces (i.e., on the top and on the bottom of the membrane, as well as in the holes) as shown in the inset of Fig. 2(b).¹¹ The Al₂O₃ thickness $d_{\text{Al}_2\text{O}_3}$ is systematically increased as in the experiment (0.9 nm/ALD step). Both the experimental and simulated data can be fitted with the same linear relations

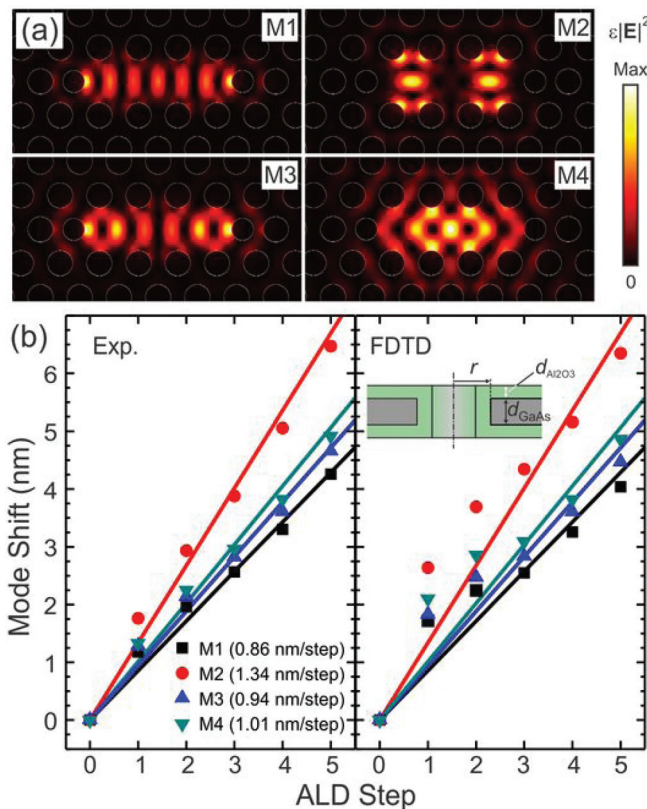


FIG. 2. (Color online) (a) Calculated electric field intensity profiles of the TE-like modes M1–M4. (b) The experimentally observed and numerically simulated mode shifts. For each mode, the experimental and simulation data are simultaneously fitted with linear functions and the obtained slopes are shown in the lower right inset of the left graph. The upper inset of the right graph shows a cross-sectional schematic of the GaAs slab with a hole. Geometry changes due to ALD coating with Al₂O₃ are marked.

and show the same behaviors. The mode M2 shows the maximum wavelength shift of 1.34 nm/step while the others (M4, M3, and M1) show increasingly smaller shifts (1.01, 0.94, and 0.86 nm/step). The larger shift of M2 can be understood by considering the mode profile shown in Fig. 2(a). Due to the fact that the mode M2 largely overlaps with the air-hole interface, it is the most sensitive to interface changes induced by the coating. We note that the field patterns of the modes M1 and M3 resemble Fabry-Perot modes, so that their spectral position is mostly influenced by the distance between the small holes next to the defect. Our FDTD simulations show a good agreement with the experiment when the ALD coating thickness is more than 1.8 nm (>2 ALD steps). The discrepancy between experiment and FDTD results at initial ALD coating (1–2 steps) might be due to the difficulty to accurately determine the average refractive index from the subpixel structure.¹⁵

C. Effects of geometric variations on the mode shift

Apart from the L3 PhC nanocavity with the parameters shown in Fig. 1, we also performed the experiment on L3 cavities with other nominal parameters. Figure 3 shows

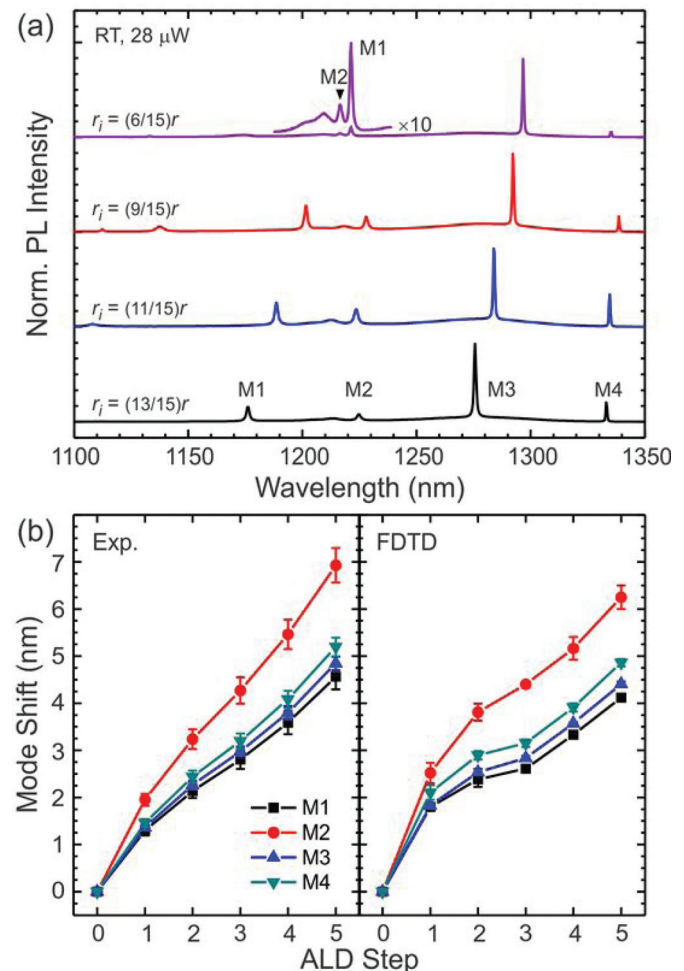


FIG. 3. (Color online) Normalized μ -PL from L3 PhC nanocavities with different size of the hole next to the cavity [see inset of Fig. 1(a) for the definition of r_i and r]. (b) The experimentally observed and numerically simulated mode shifts. The data from different cavities are collectively shown as average values. The error bars are standard deviations.

spectra for as-processed L3 PhCs with different radius r_i of the holes next to the defect [see the inset of Fig. 1(a)]. The spectra show mainly four peaks (M1–M4), where M3 has always maximum intensity due to its energy overlap with the maximum of the ground state emission of the QDs. Obviously from these spectra, the modes M1 and M3 show large and systematic redshifts when the r_i is decreased. This is due to the fact that these two modes are largely influenced by the two holes next to the confining region: As the hole radius decreases, the cavity length increases, thus producing a redshift of the resonant wavelengths. The modes M1 and M4 show slight variation (with no systematic shift). Note that for the smallest hole radius [$r_i = (6/15)r$] the mode M1 and M2 interchanges their sequence. This has been observed previously¹⁷ and it has been confirmed by our FDTD simulation. Polarization-dependent measurements could be used to further confirm the mode identification.^{17,19}

By performing Al_2O_3 ALD coating steps on these L3 PhCs, all optical modes redshift. The results are summarized in Fig. 3(b). The data points represent the average values of the shifts obtained from these four L3 PhCs and the error bars correspond to the standard variation. The mode M2 always shows the maximum shift while the effect of ALD coating on other modes (M4, M3, and M1) progressively decreases. The FDTD can reproduce these shifts as shown in the right part of Fig. 3(b). The slight deviation from a linear trend at the initial coating steps (1–2 steps) is again observed in all simulations. From this experiment, we conclude that the variation of inner hole radius in the studied range [$r_i = (6/15)r - (13/15)r$] does not have significant effects on the mode shifting induced by ALD coating.

IV. LASER PROCESSING (LASER PROCESSING OF ALD COATED PHCS)

A. Laser-processing after ALD coating

The experimental method shown above can be combined with our recently developed technique which is based on *in situ* laser-assisted oxidation. The laser typically used in our μ -PL measurement can be applied to induce oxidation simply by increasing its power for a short time.⁷ As shown previously, this method transforms the surface of the GaAs layer into GaAs-oxide and thus produces a thinning of the effective slab layer thickness as well as an increase of the effective hole radii. The outcome from laser-assisted oxidation is a blueshift of the optical modes. The bottom-most spectrum in Fig. 4(a) shows the mode M3 of an L3 cavity before processing. By multiple ALD coating steps, the mode redshifts, while subsequent laser assisted oxidation produces a blueshift of the mode to the original peak position [see spectra and labeling on the right side of Fig. 4(a)]. The laser power used here (<50 mW) is limited to avoid a substantial degradation of the cavity (lowering of the Q factor) due to an increase of GaAs-oxide interface roughness as well as an increase of the density of surface states.⁷ Then, we can also further use ALD coating to redshift the emission again after laser-assisted oxidation, as shown in the 3 topmost spectra in the figure.

The shift of the mode peak in the experiment can also be well reproduced by our FDTD simulations. The open triangle

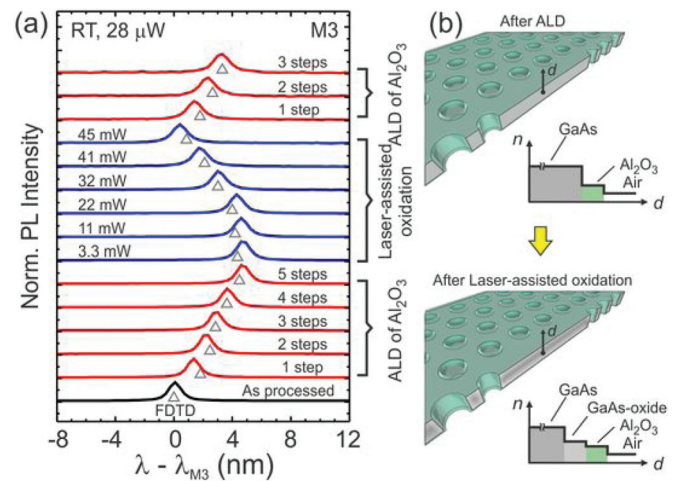


FIG. 4. (Color online) (a) A series of normalized μ -PL spectra showing the redshifts by ALD coating with Al_2O_3 , the blueshift by laser-assisted oxidation and the further redshift by additional ALD coating. The open triangles are FDTD simulation results. (b) Schematic models of a half of the L3 PhC after ALD (top) and after laser-assisted oxidation (bottom). The refractive index profiles along the vertical line are shown as insets.

shown in Fig. 4(a) is the result from the simulation, where we apply the model of laser-assisted oxidation schematically shown in Fig. 4(b), which displays schematic cross sections of a L3 PhC cavity after ALD coating. The refractive index along the thickness of the slab (from the center) is schematically plotted in the inset. Prior to laser-assisted oxidation, the PhC consists mainly of GaAs and Al_2O_3 . The thin native GaAs-oxide at the interface is assumed to be negligible. After laser-assisted oxidation, we model the GaAs-oxide formation at the interface between GaAs and Al_2O_3 . The GaAs-oxide is assumed to have a refractive index of 1.7, which is much lower than the refractive index of GaAs at this wavelength (3.09) (Ref. 20). Due to the fact that GaAs-oxide has a lower density, we relate the increase of GaAs-oxide thickness Δd_{ox} to the decrease of the GaAs thickness Δd_{GaAs} by $\Delta d_{\text{ox}} = -1.15 \Delta d_{\text{GaAs}}$. This apparently makes the slab thicker and the hole smaller. For input to FDTD, a symmetric four-layer model is considered to calculate the effective refractive index. The details of this calculation are given in the Appendix. In the FDTD, the hole radii and refractive index are simultaneously changed. A blueshift of 3.63 nm shown in Fig. 4(a) is obtained when 1.3 nm GaAs are changed into GaAs-oxide.

B. GaAs-oxide thickness

In order to gain further evidence that the mode blueshifts observed during laser processing are due to oxide formation at the $\text{Al}_2\text{O}_3/\text{GaAs}$ interface, we have performed the following experiment. First, two L3 PhCs on the same sample are coated with 8 ALD steps (4.5 nm Al_2O_3). One of the cavities is then irradiated by laser with increasing power up to 40 mW. The blueshift of the mode M3 is shown in Fig. 5. After that we dipped the sample in HCl. This step results in a peak redshift of 0.77 nm for the PhC after laser-assisted oxidation while it causes 1.33 nm blueshift for the PhC without laser-assisted oxidation treatment (see Fig. 5). The reason for

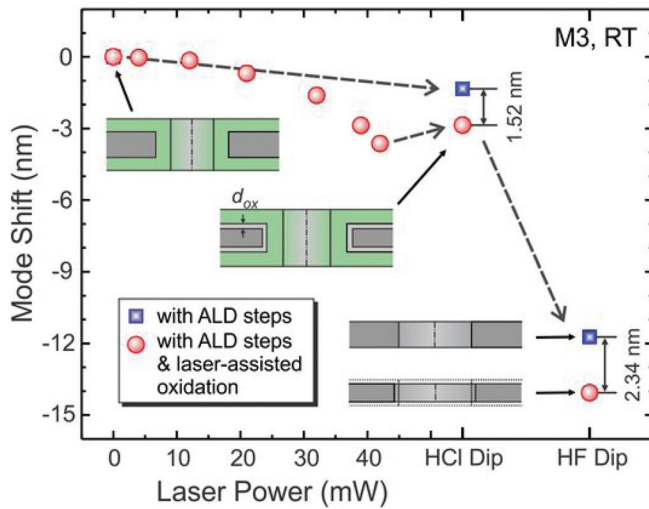


FIG. 5. (Color online) Experimentally observed mode shifts of the M3 mode initially with and without laser-assisted oxidation steps. By selective removal of Al_2O_3 and GaAs-oxide layers by HF dip (after the HCl dip) the mode peaks significantly shift. Different in this shift (2.34 nm) is contributed to the thickness of GaAs-oxide layer forming during laser-assisted oxidation (~ 1.1 nm).

the different shift is not clear but it might be due to laser-induced surface reaction of the residual material on the surface after ALD coating. However, the spectra after HCl dip of these 2 cavities still show a different shift of 1.52 nm, which indicates that the internal layer of these 2 samples are different due to the formation of GaAs-oxide in the laser-assisted oxidation sample. Finally an HF dip is used to completely remove both the Al_2O_3 and the GaAs-oxide layer without significant GaAs etching. The final HF dip step produces a blueshift of 11.7 and 14.1 nm for these two cavities (the laser-processed cavity shifts more than the other). From the FDTD simulation of these structures, the observed difference of the shifts (2.34 nm) corresponds to ~ 1.1 nm GaAs removal. This GaAs thickness is well comparable with the GaAs thickness assumed in the former experiment (Sec. IV A). Therefore, this experiment confirms that the peak shift due to laser-assisted oxidation originates mainly from the formation of GaAs-oxide layer at the interface between GaAs and Al_2O_3 .

V. CONCLUSIONS

In conclusion, we present methods to tune the spectral position of optical modes in PhC nanocavities. By *ex situ* ALD coating, we can systematically redshift the mode due to the increase of the slab thickness and the reduction of the air-hole size. We show that the degree of redshift is different for different modes due to the distinct nature of individual mode profiles. In combination with *in situ* laser-assisted oxidation, the optical modes can be blueshifted and this shift can be explained by GaAs-oxide formation at the interface between GaAs and ALD coated layer. These results can be well reproduced by our FDTD modeling including effective refractive index variation due to the change in the vertical structure.

ACKNOWLEDGMENTS

The authors gratefully acknowledge J.D. Plumhof and M. Benyoucef for their contribution to the measurement and P. Atkinson for fruitful discussions. This work was supported by the DFG (FOR 730). One of the authors (H.S. Lee) was supported by Basic Science Research Program through the National Research Foundation of Korea (NRF) funded by the Ministry of Education, Science and Technology (2010-0021189).

APPENDIX: CALCULATION OF EFFECTIVE REFRACTIVE INDEX FROM MULTILAYER STRUCTURES

The effective index theory is used to extract the effective refractive index n_{eff} for the 2D FDTD simulation.²¹ For a single slab GaAs layer, a symmetric bilayer of GaAs and air is used. The dispersion relation of the refractive index of GaAs is given by²²

$$n_{\text{GaAs}}(En) = \sqrt{7.10 + \frac{3.78}{1 - 0.18En^2} - \frac{1.97}{(30.08En)^2 - 1.0}}, \quad (\text{A1})$$

where $En = hc/\lambda$ is the emission energy, h is Planck's constant, c is the speed of light in vacuum, and λ is the free space wavelength. We now consider a slab of GaAs in air ($n_{\text{Air}} = 1$) with thickness d_{GaAs} and center at the origin of the coordinate system. By solving the standard Helmholtz equation, the lowest energy transverse (in-plane) electric field due to the vertical confinement is in the form

$$E(z) = \begin{cases} C_1 \cos(p_1 z), & 0 \leq z \leq d_{\text{GaAs}}/2 \\ C_2 \exp(-qz), & z > d_{\text{GaAs}}/2 \\ E(-z), & z < 0, \end{cases} \quad (\text{A2})$$

where C_i are constants being determined from the boundary conditions, $p_1 = (En/\hbar c)\sqrt{n_{\text{GaAs}}^2 - n_{\text{eff}}^2}$, $q = (En/\hbar c)\sqrt{n_{\text{eff}}^2 - 1}$, and z is the vertical axis. $E(z)$ equals $E(-z)$ for $z < 0$ due to the even parity of this mode. The effective index n_{eff} can be obtained by matching the boundary conditions for in-plane electric field and in-plane magnetic field at $z = d_{\text{GaAs}}/2$. After some algebraic manipulation, the following equation is obtained:

$$\tan(p_1 d_{\text{GaAs}}/2) = q/p_1. \quad (\text{A3})$$

This transcendental equation has no analytical solution. Therefore, the numerical solution of n_{eff} is extracted and put into FDTD. Note that this n_{eff} is a function of both d_{GaAs} and wavelength.

We consider a GaAs slab with thickness d_{GaAs} coated with Al_2O_3 of thickness $d_{\text{Al}_2\text{O}_3}$ and refractive index $n_{\text{Al}_2\text{O}_3}$ of 1.63. By solving the Helmholtz equation for each layer, we obtain the in-plane electric field in the form:

$$E(z) = \begin{cases} C_1 \cos(p_1 z), & 0 \leq z < d_{\text{GaAs}}/2 \\ C_2 \exp(p_2 z) + C_3 \exp(-p_2 z), & d_{\text{GaAs}}/2 \leq z < d_{\text{GaAs}}/2 + d_{\text{Al}_2\text{O}_3} \\ C_4 \exp(-qz), & z \geq d_{\text{GaAs}}/2 + d_{\text{Al}_2\text{O}_3} \\ E(-z), & z < 0, \end{cases} \quad (\text{A4})$$

where C_i are constants being determined from the boundary conditions and $p_2 = (En/\hbar c)\sqrt{n_{\text{eff}}^2 - n_{\text{Al}_2\text{O}_3}^2}$. The effective index n_{eff} can be obtained by matching two boundary conditions and getting rid of the constants, C_i . The transcendental equation is obtained.

$$\frac{p_2 [p_2 \cos(p_1 d_{\text{GaAs}}/2) \sinh(p_2 d_{\text{Al}_2\text{O}_3}) - p_1 \sin(p_1 d_{\text{GaAs}}/2) \cosh(p_2 d_{\text{Al}_2\text{O}_3})]}{p_1 [p_1 \sin(p_1 d_{\text{GaAs}}/2) \sinh(p_2 d_{\text{Al}_2\text{O}_3}) - p_2 \cos(p_1 d_{\text{GaAs}}/2) \cosh(p_2 d_{\text{Al}_2\text{O}_3})]} = q/p_1, \quad (\text{A5})$$

In case of a GaAs slab with GaAs-oxide (thickness d_{Ox} and refractive index $n_{\text{Ox}} = 1.7$) and Al_2O_3 layers, a four slab model is used. The in-plane electric field is in the form:

$$E(z) = \begin{cases} C_1 \cos(p_1 z), & 0 \leq z < d_{\text{GaAs}}/2 \\ C_2 \exp(p_2 z) + C_3 \exp(-p_2 z), & d_{\text{GaAs}}/2 \leq z < d_{\text{GaAs}}/2 + d_{\text{Ox}} \\ C_4 \exp(p_3 z) + C_5 \exp(-p_3 z), & d_{\text{GaAs}}/2 + d_{\text{Ox}} \leq z < d_{\text{GaAs}}/2 + d_{\text{Al}_2\text{O}_3} + d_{\text{Ox}} \\ C_6 \exp(-qz), & z \geq d_{\text{GaAs}}/2 + d_{\text{Al}_2\text{O}_3} + d_{\text{Ox}} \\ E(-z), & z < 0, \end{cases}$$

where C_i are constants and $p_3 = (En/\hbar c)\sqrt{n_{\text{eff}}^2 - n_{\text{Ox}}^2}$. By algebraic techniques, a lengthy transcendental equation can be obtained by matching three boundaries. The effective index, which is a function of thickness of these three layers (GaAs, GaAs-oxide, and Al_2O_3) and wavelength, can be numerically calculated. The dependency on each parameter is linearized prior to input into the FDTD simulations.

¹O. Painter, R. K. Lee, A. Schere, A. Yariv, J. D. O'Brien, P. D. Dapkus, and I. Kim, *Science* **284**, 1819 (1999).

²H. Y. Ryu, S. H. Kwon, Y. J. Lee, Y. H. Lee, and J. S. Kim, *Appl. Phys. Lett.* **80**, 3476 (2002).

³M. Lončar, T. Yoshie, A. Scherer, P. Gogna, and Q. Yueming, *Appl. Phys. Lett.* **81**, 2680 (2002).

⁴J. Vučković, and Y. Yamamoto, *Appl. Phys. Lett.* **82**, 2374 (2003).

⁵K. Hennessy, A. Badolato, A. Tamboli, P. M. Petroff, E. Hu, M. Atattüre, J. Dreiser, and A. Imamoğlu, *Appl. Phys. Lett.* **87**, 021108 (2005).

⁶A. Badolato, K. Hennessy, M. Atattüre, J. Dreiser, E. Hu, P. M. Petroff, and A. Imamoğlu, *Science* **308**, 1158 (2005).

⁷H. S. Lee, S. Kiravittaya, S. Kumar, J. D. Plumhof, L. Balet, L. H. Li, M. Francardi, A. Gerardino, A. Fiore, A. Rastelli, and O. G. Schmidt, *Appl. Phys. Lett.* **95**, 191109 (2009).

⁸S. Mosor, J. Hendrickson, B. C. Richards, J. Sweet, G. Khitrova, H. M. Gibbs, T. Yoshie, A. Scherer, O. B. Shchekin, and D. G. Deppe, *Appl. Phys. Lett.* **87**, 141105 (2005).

⁹A. Rastelli, A. Ulhaq, S. Kiravittaya, L. Wang, A. Zrenner, and O. G. Schmidt, *Appl. Phys. Lett.* **90**, 73120 (2007).

¹⁰A. Faraon, D. Englund, I. Fushman, J. Vučković, N. Stoltz, and P. Petroff, *Appl. Phys. Lett.* **90**, 213110 (2007).

¹¹X. Yang, C. J. Chen, C. A. Husko, and C. W. Wong, *Appl. Phys. Lett.* **91**, 161114 (2007).

¹²M. Francardi, L. Balet, A. Gerardino, C. Monat, C. Zinoni, L. H. Li, B. Alloing, N. Le Thomas, R. Houdré, and A. Fiore, *Phys. Status Solidi C* **3**, 3693 (2006).

¹³A. Rastelli, S. Kiravittaya, L. Wang, C. Bauer, and O. G. Schmidt, *Physica E (Amsterdam)* **32**, 29 (2006).

¹⁴A. F. Oskooi, D. Roundy, M. Ibanescu, P. Bermel, J. D. Joannopoulos, and S. G. Johnson, *Comput. Phys. Commun.* **181**, 687 (2010).

¹⁵A. Farjadpour, D. Roundy, A. Rodriguez, M. Ibanescu, P. Bermel, J. D. Joannopoulos, S. G. Johnson, and G. Burr, *Opt. Lett.* **31**, 2972 (2006).

¹⁶V. A. Mandelshtam and H. S. Taylor, *J. Chem. Phys.* **107**, 6756 (1997); *ibid.* **109**, 4128 (1998).

¹⁷A. R. A. Chalcraft, S. Lam, D. O'Brien, T. F. Krauss, M. Sahin, D. Szymanski, D. Sanvitto, R. Oulton, M. S. Skolnick, A. M. Fox, D. M. Whittaker, H.-Y. Liu, and M. Hopkinson, *Appl. Phys. Lett.* **90**, 241117 (2007).

¹⁸Y. Mizokawa, O. Komoda, and S. Miyase, *Thin Solid Films* **156**, 127 (1988).

¹⁹R. Oulton, B. D. Jones, S. Lam, A. R. A. Chalcraft, D. Szymanski, D. O'Brien, T. F. Krauss, D. Sanvitto, A. M. Fox, D. M. Whittaker, M. Hopkinson, and M. S. Skolnick, *Opt. Express* **15**, 17221 (2007).

²⁰P. A. Barnes and D. P. Schinke, *Appl. Phys. Lett.* **30**, 26 (1977).

²¹P. Yeh, *Optical Waves in Layered Media* (Wiley, New York, 2005), p. 305.

²²"Properties of Gallium Arsenide," EMIS Datareviews Series, 3rd ed., edited by M. R. Brozel and G. E. Stillman (INSPEC, London, 1996).